



ELSEVIER

Contents lists available at ScienceDirect

Data in brief

journal homepage: www.elsevier.com/locate/dib

Data Article

Data on single pulse fs laser induced submicron bubbles in the subsurface region of soda-lime glass

Shengying Lai ^{a, b}, Martin Ehrhardt ^b, Pierre Lorenz ^b, Jian Lu ^b, Bing Han ^c, Klaus Zimmer ^{b, *}^a School of Science, Nanjing University of Science & Technology, Xiaolingwei 200, Nanjing, 210094, China^b Leibniz Institute of Surface Engineering (IOM), Permoserstr. 15, 04318, Leipzig, Germany^c Advanced Launching Co-innovation Center, Nanjing University of Science & Technology, Xiaolingwei 200, Nanjing, 210094, China

ARTICLE INFO

Article history:

Received 19 December 2019

Received in revised form 15 January 2020

Accepted 20 January 2020

Available online 28 January 2020

Keywords:

Femtosecond laser

Single pulse

Bubble

Surface modification

Nonlinear absorption

Soda-lime glass

ABSTRACT

Submicron bubble formation in the subsurface range of soda-lime glass is investigated. The bubbles are induced by single femto-second laser pulse irradiation with the wavelength of $\lambda = 775$ nm, the pulse duration of $t_p = 150$ fs and the laser beam diameter of ~ 12 μm . The data shows the changes of the morphologies of the soda-lime glass after laser irradiation with different pulse energy. Moreover, the data shows the detail of the cross-section view of the bubble during the Focused ion beam (FIB) cutting. It is found that the bubbles can be formed in a rather narrow pulse energy range with the bubbles in the size of 300 nm ~ 3 μm which is much smaller than the laser beam diameter. Data presented in this article are related to the research article "Submicron bubbles/voids formation in the subsurface region of soda-lime glass by single pulse fs laser-induced spallation" [1].

© 2020 Published by Elsevier Inc. This is an open access article under the CC BY-NC-ND license (<http://creativecommons.org/licenses/by-nc-nd/4.0/>).

DOI of original article: <https://doi.org/10.1016/j.apsusc.2019.144134>.

* Corresponding author.

E-mail address: klaus.zimmer@iom-leipzig.de (K. Zimmer).<https://doi.org/10.1016/j.dib.2020.105193>2352-3409/© 2020 Published by Elsevier Inc. This is an open access article under the CC BY-NC-ND license (<http://creativecommons.org/licenses/by-nc-nd/4.0/>).

Specifications Table

Subject	Material Science Engineering
Specific subject area	Laser material processing
Type of data	Table Image Graph Figure
How data were acquired	Optical microscopy (OM; Jenaval, Carl Zeiss Jena), SEM(Ultra 55 from Carl Zeiss), AFM(Dimension Icon; Bruker), WLIM(Micromap 512 from ATOS)
Data format	Raw Analyzed
Parameters for data collection	Original defects of the soda-lime glass and chemical cleaning of the glass before laser irradiation
Description of data collection	Effects of femtosecond laser irradiation parameters on the micro structures, morphology and chemical composition in the near surface of the soda-lime glass are demonstrated via processed SEM data, AFM data as well as the EDX data.
Data source location	Dr. Zimmer, Leibniz Institute of Surface Engineering (IOM), Leipzig, Germany
Data accessibility	With the article
Related research article	Lai S, Ehrhardt M, Lorenz P et al. Submicron bubbles/voids formation in the subsurface region of soda-lime glass by single pulse fs laser-induced spallation[J]. Applied Surface Science, 2019: 144134. DOI of original article: https://doi.org/10.1016/j.apsusc.2019.144134

Value of the Data

- The data shows the changes in surface morphology of soda-lime glass with different incident laser pulse energy.
- The data will contribute to our understanding of the thermal driven and viscoplastic-mechanical processes during the bubble formation as well as ablation induced by laser irradiation.
- The data could be used for practitioner and as basic data for further research.

1. Data description

The morphologies of the soda-lime glass after laser irradiation with different laser pulse energy are shown in Fig. 1 with optical microscopy (OM) measurements. The bubbles are formed with a moving laser source while the scanning speed is 4 mm/s and the repetition rate of the laser is 1 kHz. The three kinds of morphologies characterize the three different surface conditions induced by laser irradiation: a) surface modification; b) bubble formation and d) laser ablation crater.

Table 1 shows the height or the depth of the structures, the morphologies and the profile of the measured bubbles/crater in dependence on the applied pulse energy. The sizes of the bubbles are measured by the atomic force microscopy (AFM) as well as the white light interference microscopy (WLIM). The morphologies are measured by the scanning electron microscopy (SEM). The bubbles can be obtained with the maximum height of ~500 nm in the range of the surface modification and ablation. The pulse energy that below 5.32 μJ ($F = 4.01 \text{ J/cm}^2$) can only induced the surface modification on the soda-lime glass or some small bubbles with the height below 60 nm. The glass features small bulging to the direction of the incident laser beam but the height is only several nm. When the pulse energy is higher than 5.5 μJ ($F = 4.14 \text{ J/cm}^2$), most of the laser irradiated spots show explored bubbles or ablation craters. The size of the bubbles or the ablation craters are much smaller than the laser beam diameter. From the table it can be found that with the increasing of the incident pulse energy, the bubbles' height increases too as well as the bubble diameter. But there are some fluctuations of the bubble size due to the surface condition of the soda-lime glass.

Fig. 2 shows the FIB cutting process of the bubble and the cross-section view of the bubble. A thin Pt film ~1.5 μm is deposited on the glass surface in order to protect the surface structures as well as the

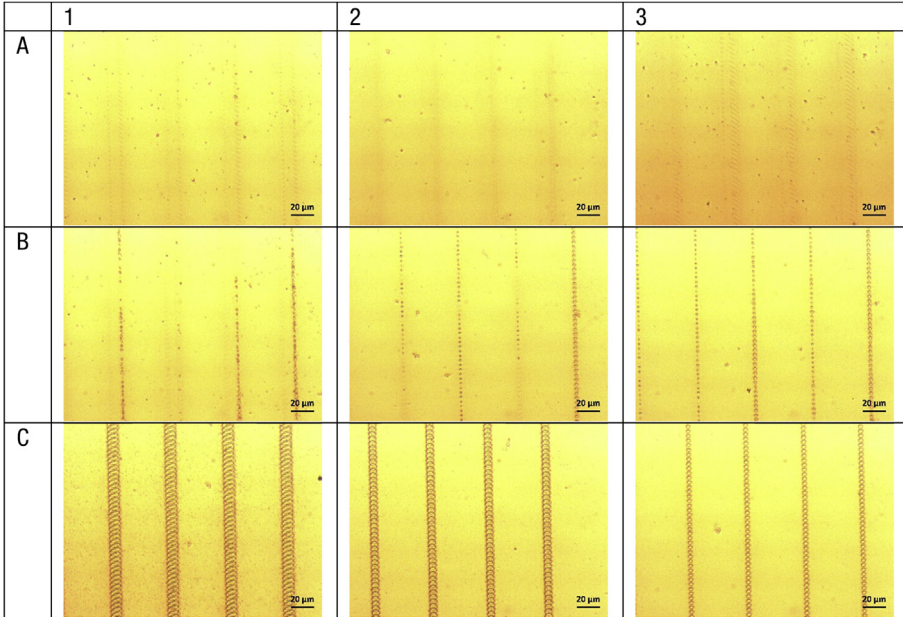


Fig. 1. OM images of the soda-lime glass after laser irradiation with different incident laser pulse energy, row A surface modification (The pulse energy is the same from column 1 to 3, $\bar{E} = 5.14 \mu\text{J}$, $F = 3.87 \text{ J/cm}^2$); row B bubble formation (The pulse energy is the same from column 1 to 3, $\bar{E} = 5.32 \mu\text{J}$, $F = 4.01 \text{ J/cm}^2$) and row C ablation ($\bar{E} = 6.17, 5.82$ and $5.52 \mu\text{J}$ ($F = 4.65, 4.38$ and 4.16 J/cm^2) from column 1 to 3). The laser scanning is 4 mm/s, the repetition rate is 1 kHz, the laser beam diameter is $\sim 12 \mu\text{m}$.

bubble. The bubble is fabricated with $5.32 \mu\text{J}$ ($F = 4.01 \text{ J/cm}^2$). From the cross-section view of the bubble it can be clearly seen that the bubble inside is a hollow ellipsoid with an upper shell of about 100 nm in thick. This thickness shows constant in relation to the other bubble shell with damaged or flipped bubbles presented in Ref. [1].

Fig. 3 sketches the laser irradiation setup as well as the measurement of the laser signal by the oscilloscope. The oscilloscope is connected to the photodiode which is fixed near the beam path to detect the scatter light. Fig. 4 shows the probability of the bubble formation at a certain pulse energy range from $5.5 \mu\text{J}$ to $5.6 \mu\text{J}$.

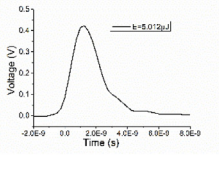
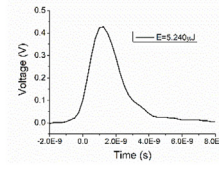
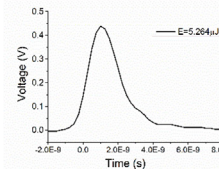
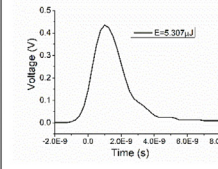
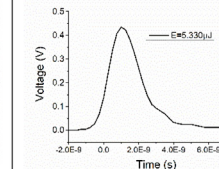
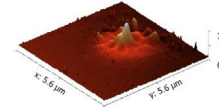
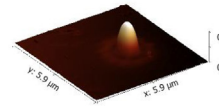
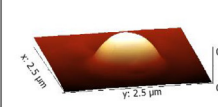
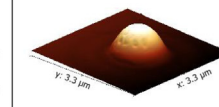
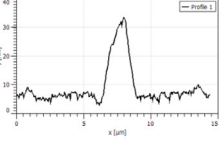
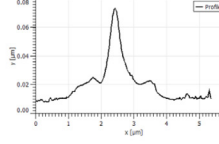
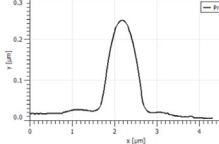
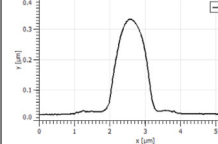
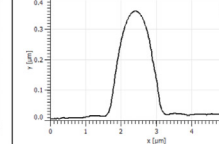
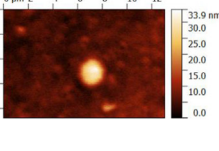
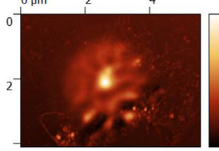
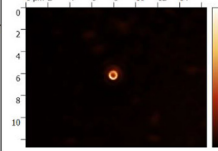
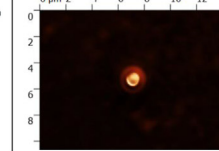
2. Experimental design, materials, and methods

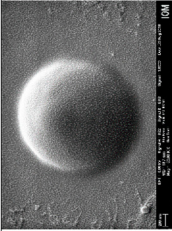
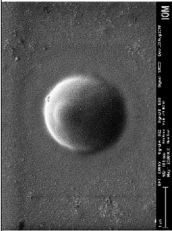
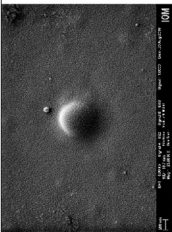
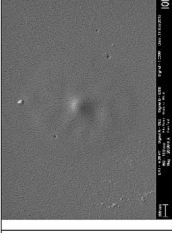
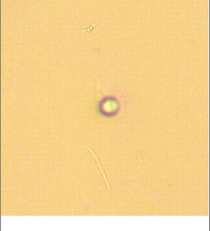
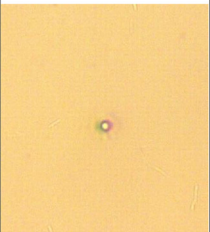
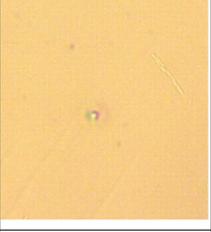
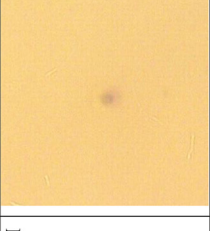
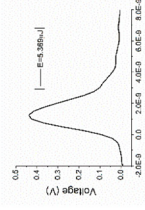
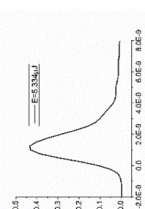
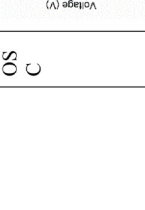
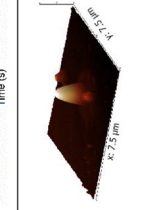
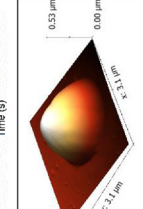
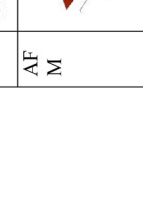
2.1. Experimental design

A linear polarized femtosecond laser with a wavelength of 775 nm, a pulse duration of 150 fs, and a pulse repetition of 1 kHz is used in this study. The laser beam with a Gaussian profile is focused on the surface of the glass with a single lens having a focal length of 60 mm. The laser spot radius was determined to be $r_g = 6.5 \pm 0.5 \mu\text{m}$. The samples are irradiated in a pulse energy range of $E = 3.00$ ($F = 2.26 \text{ J/cm}^2$) $\sim 20 \mu\text{J}$ ($F = 15.1 \text{ J/cm}^2$) with a scanning speed of 4 mm/s and then irradiated with single laser pulses arranged in a line as shown in Fig. 1. After that, a spacing of more than $20 \mu\text{m}$ is used for single pulse irradiation to avoid the influence of the overlap by multi-pulse irradiation with the laser pulse energy varied from 4.6 ($F = 3.47 \text{ J/cm}^2$) to $6.6 \mu\text{J}$ ($F = 4.97 \text{ J/cm}^2$).

Table 1

The formed three kinds of surface morphologies including modification, bubbles formation and ablation independence on the incident pulse energy and their relative measurements including pulse signal measured by the oscilloscope (OSC), the profile and 3D topography measured by AFM, WLIM, SEM, OM and the related parameters.

	Surface modification	Small bubble	Increasing bubble size with increasing pulse energy		
Number	1	2	3	4	5
OSC					
AFM					
Profile					
WLIM					

SE M									
OM									
Parameter	<p>E = 5.012 μJ F = 3.78 J/cm^2 H = 17 nm</p> <p>E = 5.240 μJ F = 3.95 J/cm^2 H = 64 nm</p> <p>E = 5.264 μJ F = 3.97 J/cm^2 H = 237 nm</p> <p>E = 5.307 μJ F = 4.00 J/cm^2 H = 312 nm</p> <p>E = 5.330 μJ F = 4.02 J/cm^2 H = 346 nm</p>								
Numer	Increasing bubble size with increasing pulse energy								
OS	6	7	8	9					
									
AFM									

Profile					<p>E = 5.334 μJ F = 4.02 J/cm^2 H = 420 nm</p>
Profile					<p>E = 5.388 μJ F = 4.06 J/cm^2 H = 385 nm</p>
Profile					<p>E = 5.44 μJ F = 4.10 J/cm^2 H = -180 nm</p>

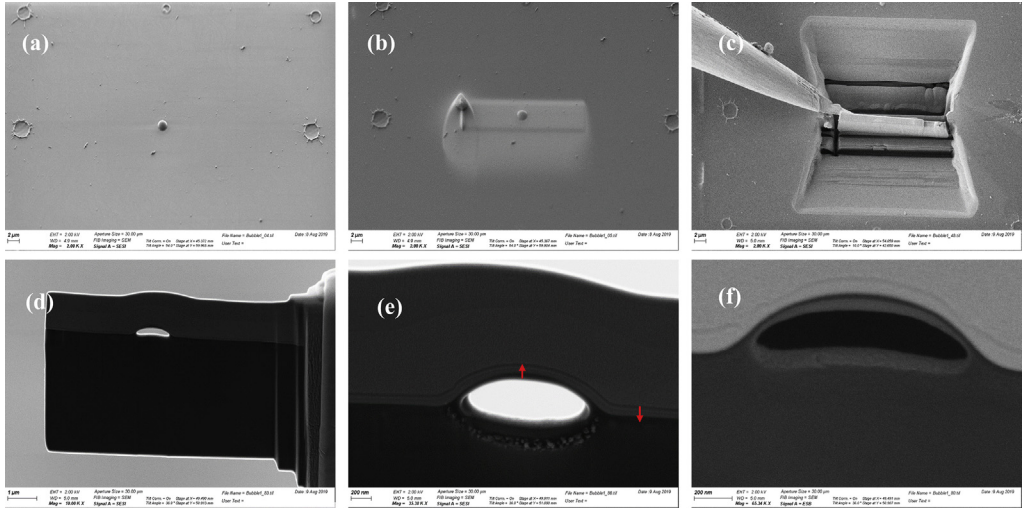


Fig. 2. The FIB cutting process of the bubble, the arrows in the image shows the border of the bubble from the upper shell of the bubble to the platinum film and the border of the glass substrate to the platinum film.

2.2. Materials

The material used in this experiment is microscope slides (extra white soda-lime glass, Menzel Thermo Scientific) with a thickness of 1 ± 0.1 mm. The composition of the glass is 72% SiO₂, 14% Na₂O, 6% CaO, 4% MgO, 1% Al₂O₃, 1% K₂O and further additives in small amounts. The samples are cleaned in an ultrasonic bath with isopropanol and dried by nitrogen gas flow. However, each piece of the sample will have some difference on the composition based on the fabrication process which may result in the bubble size deviation in [Table 1](#).

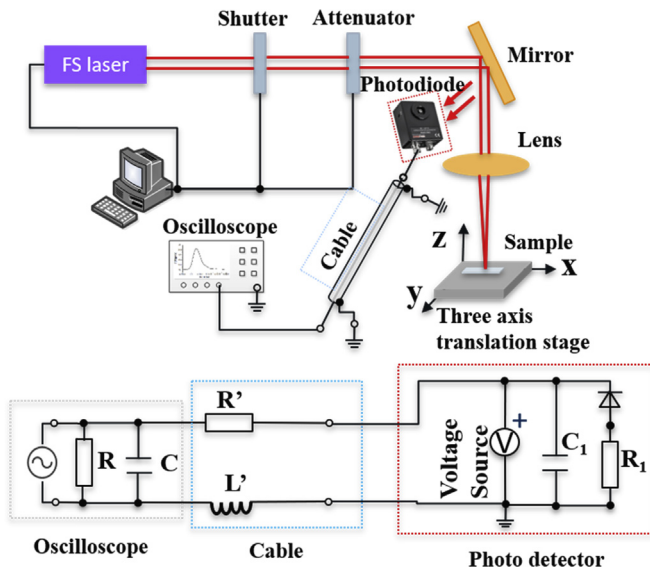


Fig. 3. Sketch of experimental setup for single pulse energy measurement and the equivalent circuit for detecting the laser signal and the measured voltage signal in correlation of the laser pulse energy.

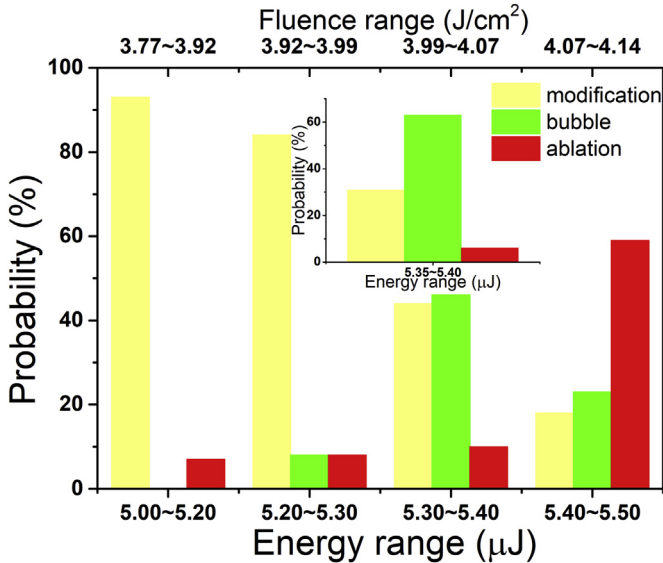


Fig. 4. The probability of the appearance of the three different morphologies in dependence on the incident pulse energy.

2.3. Methods

In the experimental design it has been mentioned that arrays of laser spots have been built with single pulse laser irradiation ordered in rows of nominal equal irradiations and varying the fluence from row to row. At this condition, a photodiode (THORLABS, DET 10 A/M, 200–1100 nm) is fixed near the beam path to measure the scatter light signal during the laser irradiation for each laser pulse. An oscilloscope is used to record the voltage from the photodiode so that the single pulse laser energy can be recorded. Due the extremely short pulse duration (150 fs) and the inductive and capacitive properties of the measuring circuit, the electrically recorded pulse is not proportional to the temporal pulse power but proportional to the pulse energy. As the impedance of the devices can be considered as constant, the integral value of the voltage measured by the oscilloscope provides the laser pulse energy. The equivalent circuit is shown in Fig. 3.

Before the laser irradiation process, an energy meter (Coherent) is placed in the laser beam path between the mirror and the focus lens. The pulse energy is measured by the energy meter while the photodiode connected to the oscilloscope detects the scatter light at the same time. After that we calculate the average pulse energy of the scores of the pulse energy Ea as well as the relative integral value Ia detected from the oscilloscope. We define $k = Ea/Ia$ for normalization so that we can get the scatter light signal and its integral value I_i . Therefore, $E_i = k * I_i$. Therefore, the relationship between the pulse energy and the scatter light detected by the photodiode is established.

From Fig. 1 in row B it can be found that at the bubble formation range, there still have some fluctuations of the pulse energy which result in the morphology fluctuation and make the bubbles' formation occur in a random probability. From the hundreds spots the probability of the formation of the different surface morphologies (checked by SEM) in dependence on the laser pulse energy has been summarized in Fig. 4. The bubbles appear in the energy range of 5.20 ($F = 3.92 \text{ J/cm}^2$) ~5.30 μJ ($F = 3.99 \text{ J/cm}^2$) but only with a rather low probability less than 10% but almost all the surface conditions feature the modification. However, when the pulse energy increases to 5.3 ($F = 3.99 \text{ J/cm}^2$) ~5.4 μJ ($F = 4.07 \text{ J/cm}^2$), there is an almost 50% probability with the bubble formation. Moreover, in the range of 5.35 ($F = 4.03 \text{ J/cm}^2$) ~5.40 μJ ($F = 4.07 \text{ J/cm}^2$), more than 60% probability can the laser induced bubbles. Therefore, we take the nearly energy range that can generate the bubbles with 50% probability

to be the threshold of the bubbles' formation, and in the range of 5.35 ($F = 4.03 \text{ J/cm}^2$) ~5.40 μJ ($F = 4.07 \text{ J/cm}^2$), the bubbles can be generated stably. When the energy increases, the probability of the bubble formation decreases while the ablation probability increases.

The bubbles are induced by single fs laser pulse, so that the incubation effect can be neglect in this condition while the multiphoton absorption process must be considered during the laser irradiation. From the experimental results it can be found that the bubbles are all smaller than the Gaussian beam radius. The multiphoton absorption induced bubbles' size r_{MP} can be estimated theoretically according to function (1) based on the Gaussian distribution when the incident energy threshold is higher than the formation threshold [2]. Here, r_R is the actual Gaussian beam diameter and n is the photon number for the multiphoton absorption. Therefore, for different number of photon absorption such as 2, 3 and 4, the effective interaction diameter can be estimated for 2, 1.6 and 1.4 μm which is in correlation with the bubble size shown in Table 1.

$$r_{MP} = \frac{r_R}{\sqrt{n}} \quad (1)$$

The morphological measurements are performed using scanning electron microscope (SEM) and atomic force microscope (AFM). The composition in the near surface of the bubble is measured by SIMS and EDX.

Acknowledgments

The authors wish to acknowledge the help of Ms. I. Haferkorn for the SEM measurements, Mrs. A. Mill for the FIB preparation and Dr. J. Bauer for EDX analysis. This work was financially supported in parts by the Deutsche Forschungsgemeinschaft (DFG) (Zi660/17-1) and the "National Natural Science Foundation of China for International (Regional) Cooperation Research Project (No. 11761131015)",.. Further, the National Natural Science Foundation of China (No. 11774176) and the China Scholarship Council provide financial support.

Conflicts of Interest

The authors declare that they have no known competing financial interests or personal relationships that could have appeared to influence the work reported in this paper.

References

- [1] S. Lai, M. Ehrhardt, P. Lorenz, et al., Submicron bubbles/voids formation in the subsurface region of soda-lime glass by single pulse fs laser-induced spallation, *Appl. Surf. Sci.* (2019) 144134, <https://doi.org/10.1016/j.apsusc.2019.144134>.
- [2] K. Sugioka, Progress in ultrafast laser processing and future prospects, *Nanophotonics* 6 (2) (2017) 393–413, <https://doi.org/10.1515/nanoph-2016-0004>.